Generalist versus Specialist Self-Replicators

Komáromy, Dávid; Monzón, Diego M; Marić, Ivana; Monreal Santiago, Guillermo; Ottelé, Jim; Altay, Meniz; Schaeffer, Gaël; Otto, Sijbren

Published in:
Chemistry – A European Journal

DOI:
10.1002/chem.202303837

Publication date:
2024

Chemistry
A European
Journal

Chemistry Europe
European Chemical Societies Publishing

Accepted Article

Title: Generalist versus Specialist Self-Replicators

Authors: Dávid Komáromy, Diego M. Monzón, Ivana Marić, Guillermo Monreal Santiago, Jim Ottelé, Meniz Altay, Gaël Schaeffer, and Sijbren Otto

To be cited as: *Chem. Eur. J.* **2024**, e202303837

Link to VoR: https://doi.org/10.1002/chem.202303837

WILEY VCH

10.1002/chem.202303837

WILEY-VCH

FULL PAPER

Generalist versus Specialist Self-Replicators

Dávid Komáromy, [a] Diego M. Monzón, [b] Ivana Marić, [a] Guillermo Monreal Santiago, [a] Jim Ottelé, [a] Meniz Altay, [a] Gaël Schaeffer, [a] and Sijbren Otto*[a]

Abstract: Darwinian evolution, including the selection of the fittest species under given environmental conditions, is a major milestone in the development of synthetic living systems. In this regard, generalist or specialist behavior (the ability to replicate in a broader or narrower, more specific food environment) are of importance. Here we demonstrate generalist and specialist behavior in dynamic combinatorial libraries composed of a peptide-based and an oligo(ethylene glycol) based building block. Three different sets of macrocyclic replicators could be distinguished based on their supramolecular organization: two prepared from a single building block as well as one prepared from an equimolar mixture of them. Peptide-containing hexamer replicators were found to be generalists, i.e. they could replicate in a broad range of food niches, whereas the octamer peptide-based replicator and hexameric ethyleneoxide-based replicator were proven to be specialists, i.e. they only replicate in very specific food niches that correspond to their composition. However, sequence specificity cannot be demonstrated for either of the generalist replicators. The generalist versus specialist nature of these replicators was linked to their supramolecular organization. Assembly modes that accommodate structurally different building blocks lead to generalist replicators, while assembly modes that are more restrictive yield specialist replicators.

Introduction

Chemistry, having expanded its scope “beyond the molecule” (supramolecular chemistry),[1] has been recently coined “the central science”, [2] i.e. the discipline that can explain and possibly reconstruct the transition from non-living to living matter.[3] One approach, prebiotic systems chemistry[4–9] aims at *reconstructing* the formation of biomolecules and the simplest cellular entities on early Earth. An alternative approach aims at *constructing* minimal living systems stepwise from molecules which were not necessarily present on early Earth, nor necessarily used in current biochemistry. The requirements of a minimal living system can be defined in numerous ways;[10,11] one set of prerequisites,[12,13] agreed on by a vast part of the scientific community, entails (i) self-replication (autocatalytic subcomponent self-assembly and synthesis), [14–22] (ii) compartmentalization (spatial segregation of certain parts of the system, enabled by membranes or other means of confinement), [23–31] (iii) metabolic activity (the system’s ability to harness energy from the environment and to synthesize its own components) [32,33] (iv) out-of-equilibrium operation (necessity of a constant inflow of material and/or energy for the system to operate)[34–42] and (v) open-ended Darwinian evolution (continuous evolutionary innovation by formation of mutations and selection of mutants that can persist the best in a given environment).[43–46]

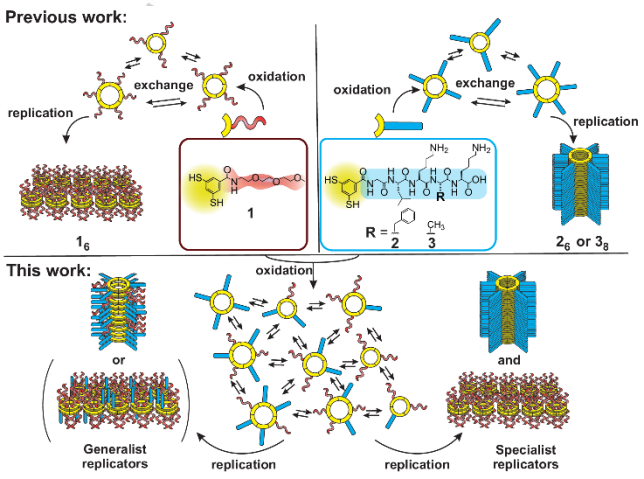

Scheme 1. Dynamic Combinatorial Chemistry of a System Composed of Oligo(ethylene oxide)-Conjugated Dithiol Building Block **1** and Peptide-Conjugated Dithiol Building Blocks **2** and **3**. In previous work we showed how a DCL made from ethyleneoxide-functionalized building blocks **1** gives rise to self-replicating hexameric macrocycles driven by their assembly into sheet-like aggregates. In contrast, peptide-functionalized building blocks **2** and **3** yield hexamer or octamer macrocycles, respectively, driven by their assembly into fibers. In this work we explore the behavior of DCLs made from binary mixtures of ethyleneoxide- and peptide-functionalized building blocks yielding specialist or generalist self-replicators, depending on the mode of assembly.

Whereas the first four traits can be realized and studied in single self-replicating molecules, the last one necessarily requires a network[47] of different competing[48] or cooperating[49,50] replicators. Whether replicators compete or can cooperate, depends on whether they feed on different food niches, one can distinguish specialist (monophagous) and generalist (polyphagous) replicators. Specialists can only thrive in narrow, non-overlapping food niches, with the evolutionary advantage of being able to persist in this specific food niche better than competing species. In contrast, generalists can feed on wider food

[a] Dr. Komáromy, Dr. I. Marić, Dr. G. Monreal Santiago, Dr. J. Ottelé, Dr. M. Altay, Dr. G. Schaeffer and Prof. Dr. S. Otto
University of Groningen, Centre for Systems Chemistry, Stratingh Institute, Nijenborgh 4, 9747 AG, Groningen, The Netherlands
E-mail: s.otto@rug.nl
Homepage: www.otto-lab.com
[b] D. M. Monzón
Instituto de Bio-Orgánica "Antonio González" (IUBO-AG), Departamento de Química Orgánica, Universidad de La Laguna, Avda. Astrofísico Fco. Sánchez, 38206, San Cristóbal de La Laguna, Santa Cruz de Tenerife, Spain

Supporting information for this article is given via a link at the end of the document.

10.1002/chem.202303837

niches, and are thus likely to be more adaptable towards change in the environment. [51] Moreover, open-endedness requires a vast structural space that replicators can (partially) explore on their way toward complexification.[13] In the context of de novo replicators constructed from simple molecules this requirement has two aspects: First, the amount of molecular information (building block sequence) passed on from generation to generation should increase in the course of evolution. Second, the supramolecular structure of the competing replicators might differ vastly, resulting in different resilience towards change in environmental conditions.[37] The diversification required for open-ended evolution is likely to benefit from the presence of generalist replicators as specialist ones are more likely to occupy only a small portion of the possible chemical space. At the same time specialist replicators are more likely to stably co-exist with other specialist replicators as they rely on smaller and more defined food niches. Cooperation between such co-existing replicators can aid in overcoming Eigen's paradox.[52] Thus, whether self-replicators are specialists or generalist has important evolutionary implications.

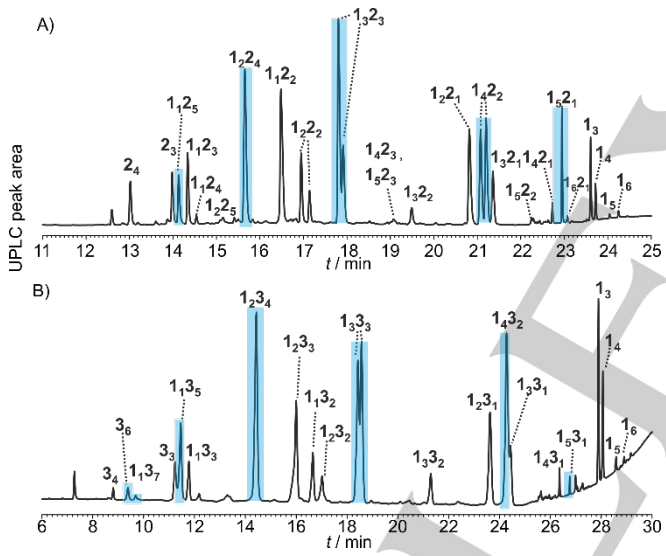

Figure 1. UPLC chromatogram of DCLs prepared from equimolar amounts of A) **1** and **2** ([**1**] = [**2**] = 2.0 mM) in aqueous borate buffer (50 mM, pH = 8.5) after 8 days of stirring; B) **1** and **3** ([**1**] = [**3**] = 2.0 mM) in aqueous phosphate buffer (50 mM, pH = 8.5) after 4 days of stirring. Self-replicating hexamers are marked with blue stripes. We observed that the emergence of $\mathbf{3_8}$ occurs more reliably in phosphate buffer than in borate buffer, hence the use of phosphate buffer in (**1**+**3**)-based systems.

Our approach[53] toward synthetic self-replicators is based on dynamic covalent chemistry[54–56] of thiols and disulfides.[57] Previously, we used peptide-dithiol conjugates such as building blocks **2** or **3**[58,59] (see Scheme 1), which, upon stirring in aqueous solution in air, first form a dynamic combinatorial library (DCL) of macrocyclic disulfides. One of these species (hexamer $\mathbf{2_6}$ and octamer $\mathbf{3_8}$, respectively) is able to autocatalytically enhance its own formation from its building blocks (i.e. self-replicate), by self-assembling into fibrous stacks, stabilized by interactions between the peptide chains which form β-sheet structural motifs.[60] Stirring of the solutions results in breakage of the fibers, thereby redoubling the number of catalytic fiber ends, enabling exponential self-replication.[61] Notably, this method yielded synthetic systems capable of exhibiting biologically relevant behavior, such as induced replication,[62–64] speciation,[65] history dependence[66] or parasitism.[67] More recently, we reported self-replicator $\mathbf{1_6}$,[68] based on oligo(ethylene oxide)-conjugated dithiol **1**, which self-assembles into densely packed nanoribbons (held together mainly by hydrophobic effects) instead of β-sheet fibers.

It remains unclear what governs whether replicators are specialists or generalists. Here we describe our attempts to shed light on this issue. We studied the emergence of self-replicators from mixtures of **1** and **2**, as well as from **1** and 3, first characterizing the size and building-block distribution of the resulting macrocycles at the molecular level, followed by studying the structure of their supramolecular assemblies. We then probed, through cross-seeding experiments, to which extent the different replicators can grow from building block mixtures with compositions different from the ones that they emerged from, thereby probing whether the different replicators are specialists or generalists. We found that the supramolecular organization of the replicators plays an important role. Within the range of building blocks studied, replicators held together by relatively strong intermolecular interactions behaved as generalists, whereas those held together by weaker interactions behaved as specialist as they failed to replicate when offered a food niche different from the original one.

Results and Discussion

Self-replicating mixed macrocycles emerge from mixed DCLs. DCLs composed of building blocks **1** and **2** or **1** and **3** seemed promising candidates to investigate the specialist-generalist dichotomy for several reasons. First, the markedly different binding strengths within the assemblies (strong, directional beta-sheet interactions vs. weaker, nondirectional hydrophobic effect) were expected to lead to different propensities of the replicators to incorporate precursor molecules when competing for resources. Second, peptide-only systems, even if composed of multiple building blocks, display the same fiber morphology, and thus remain restricted to a small portion of the possible assembly space. In contrast, possible mixing with the markedly different building block **1** could enable the formation of new nanoscale morphologies, thereby expanding the explorable structural space, which, in turn, could facilitate the formation of generalist replicators.

10.1002/chem.202303837

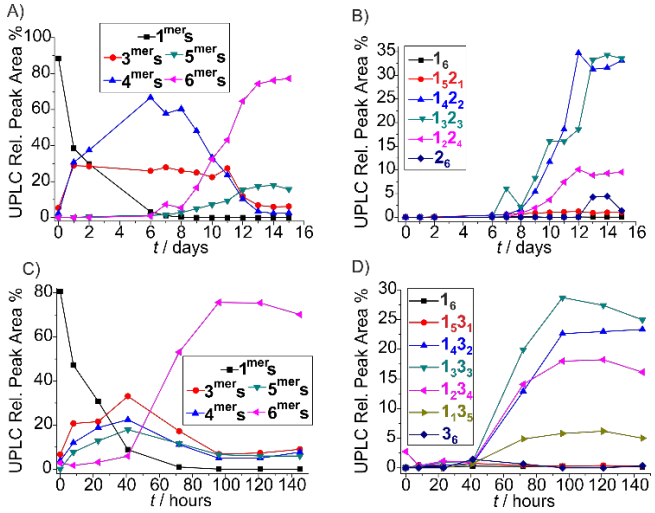

Figure 2. Time evolution of (A,C) differently sized oligomers and (B,D) different hexamers in stirred DCLs prepared from equimolar amounts of (A,B) **1** and **2** ([**1**] = [**2**] = 2.0 mM) in aqueous borate buffer (50 mM, pH = 8.5) (C,D) **1** and **3** ([**1**] = [**3**] = 2.0 mM) in aqueous phosphate buffer (50 mM, pH = 8.5).

First, we studied the behavior of mixtures composed of buildings blocks **1** and **2**. Oxidation of an equimolar mixture of **1** and **2** in aqueous borate buffer (50 mM, pH = 8.2) by air in the absence of agitation resulted in a DCL composed mainly of mixed trimers and tetramers with minor amounts of pentamers and hexamers present (Figure S55A). In stirred solution, mixed hexamers suddenly emerged after ca. 8 days (Figure 1A), whereas in the absence of stirring, trimers and tetramers remained the main components even after 14 days. Similar behavior was observed for the (**1**+**3**)-system (Figure 1B, Figure S55B). Notably, in this case, not even traces of octamer replicators (formed from pure **3** when in isolation) could be observed.

Detailed study of the kinetics of oligomer formation showed a lag phase followed by a sudden growth period for hexamers (as well as for pentamers in the (**1**+**2**)-system), characteristic for self-replicators (Figure 2A, C). In order to confirm the autocatalytic nature of hexamer growth, seeding experiments were carried out. A pre-oxidized, non-agitated DCL (food) prepared from equimolar amounts of building blocks **1** and **2** ([**1**] = [**2**] = 2.0 mM) was treated with 15 mol% of a mixture of hexamers (seed) prepared from a DCL with the same composition. In the seeded sample, immediate growth of the corresponding hexamers was observed, while in the unseeded sample, hexamer growth started only after a lag phase of ca. 50 hours (Figure S57 and Figure 7C, *vide infra*). Similar experiments were carried out for the (**1**+**3**)-system (Figure 7F). These results show that the ensemble of the mixed hexamers prepared from an equimolar mixture of **1** and **2** are self-replicators (abbreviated as (**1+2**)$_6$). Also mixed hexamers (**1+3**)$_6$ can be regarded as a distinct set of self-replicators. Additionally, transmission electron microscopy (TEM) experiments (Figure S58, S59) showed the presence of nanoscale fibers for both (**1+2**)$_6$ and (**1+3**)$_6$ (laterally associated ones in the latter case). We conclude that the ensemble of mixed hexamers exhibits similar properties to the one-component replicators, regarding their kinetics of formation as well as their supramolecular structure.

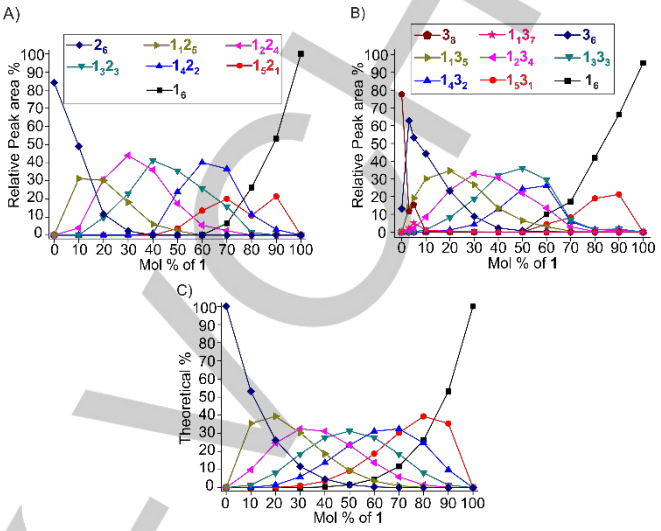

Figure 3. Relative distribution of hexamer and octamer replicators in mixed DCLs prepared from A) **1** and **2** ([**1**] + [**2**] = 4.0 mM) in aqueous borate buffer (50 mM, pH = 8.5) B) **1** and **3** ([**1**] + [**3**] = 4.0 mM) in aqueous phosphate buffer (50 mM, pH = 8.5), as the function of mol% **1**. C) Theoretical distribution of hexamers as the function of mol% **1**, based on a binomial probability of building block incorporation in the various hexamers. Note that the presence of isomeric hexamers is evident, and we cannot not exclude that their replication properties are different. However, as it is far from trivial to separately quantify the different isomers, we treated them together in this study.

Mixed self-replicators emerge as one set of species. Next, we investigated if certain replicators emerged from the corresponding monomers in different amounts than expected from the statistical (binomial) distribution. Such behavior would enable us to classify these replicators as a set distinct from other ones; the resulting classification would then enable the comparison of the different replicator sets regarding their food niche specificity.

To this end, we prepared mixed DCLs from **1**+**2** and **1**+**3** with a total building block concentration kept at 4.0 mM, containing increasing amounts of **1**. Moreover, in the (**1**+**3**)-system, we also prepared DCLs with very low molar fractions (<10 mol%) of **1** in order to study the effect of stoichiometry on the formation of octamer replicators in detail. DCLs containing the monomers in different stoichiometric ratios were stirred while exposed to air until the library composition showed no further change and the DCL members were exclusively hexamers (or octamers in the (**1**+**3**)-system). UPLC analysis (Figure 3A-B, Figure S60-S61) showed that the distribution of the relative amounts of hexamers was close to statistical (i.e. binomial distribution based on the corresponding monomer composition, Figure 3C). Notably, the relative amount of octamer **3**$_8$ decreased rapidly in the presence of even minute amounts of **1** (0-10 mol%, Figure S61A-D) and the corresponding building-block material was incorporated into the **1**$_n$**3**$_{6-n}$ mixed hexamers. Interestingly, the hexamer **3**$_6$ formed in

10.1002/chem.202303837

substantial amounts between 3 and 30 mol% **1**, although, octamer $\mathbf{3}_8$ is formed when starting from only building block **3**. [59] The only mixed octamer present in detectable although minor amounts (< 6 mol%) was $\mathbf{1}_1\mathbf{3}_7$ (Figure S61B-C). These results indicate that the stoichiometry was more strongly dictated by **1** than by **3**.

These findings show that the two building blocks are incorporated into the various hexamers with the same probability. In other words, there is no specific hexamer whose formation is thermodynamically or kinetically preferred compared to the others. Thus, based solely on stoichiometry, we could not separate the replicators into distinct sets.

Supramolecular properties show sudden phase transition behavior, allowing the distinction between replicator sets. Next, we examined how the morphological properties of the system change as a function of stoichiometry. Specifically, we were interested whether, by increasing the concentration of one building block at the expense of the other, the transition from one supramolecular structure to another is gradual or characterized by a sudden phase change. In the latter case, we could classify the replicators formed by different building block stoichiometries, into distinct sets. Furthermore, as replication kinetics (i.e. autocatalytic activity) can strongly depend on the dimensions and the nature of the formed assemblies,[69,70] the supramolecular structure might strongly influence the replicators' ability to sequester different food molecules and consequently also the food niches in which the replicator set is able to grow.

First, thioflavin T (ThT) and Nile Red fluorescence assays were used in parallel to examine the hexamer assemblies formed from DCLs with increasing amounts of **1** (Figure 4). On the one hand, the β-sheet structural motif, characteristic for the peptide replicator fibers, can be easily detected by the enhanced fluorescence of ThT at 480 nm, caused by intercalation of the ThT molecule between the peptide chains. On the other hand, Nile Red shows enhanced fluorescence in lipophilic microenvironments[71] and thus stains the nanoribbons composed of $\mathbf{1}_6$, as shown previously.[68] These spectral features are expected to be mutually exclusive in the present case: $\mathbf{1}_6$, assemblies do not contain β-sheet motifs due to the absence of peptide chains, whereas the interior of peptide fibers is expected to be much more polar than that of the nanoribbons, due to the high local concentration of amide bonds (*vide infra*).

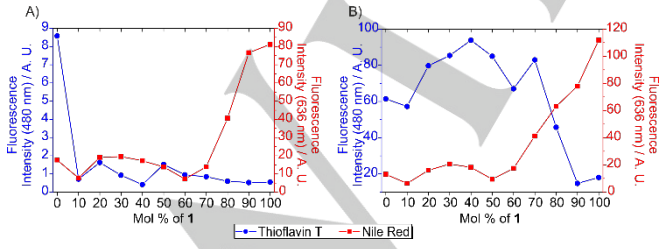

Figure 4. Maximum thioflavin T (blue trace) and Nile Red (red trace) intensities of stirred DCLs prepared from building blocks A) **1** and **2** ([**1**] + [**2**] = 4.0 mM) B) **1** and **3** ([**1**] + [**3**] = 4.0 mM) with increasing molar percentage of **1**.

Our results show that (i) The emission intensity in the Nile Red assay was 6 times higher for $\mathbf{1}_6$ than for $\mathbf{2}_6$ and $\mathbf{3}_8$, whereas the intensities measured in the ThT assay were ca. 17 and 4 times lower for $\mathbf{1}_6$ than for $\mathbf{2}_6$ and $\mathbf{3}_8$, respectively. These results indicate that the two assays are indeed mutually exclusive, as expected. (ii) In the (**1**+**2**)-system, both assays showed an abrupt change in fluorescence intensity at compositions close to that corresponding to the pure replicators (Figure 4A): ThT fluorescence dropped to a value 8 times lower at 10 mol % of **1**, whereas Nile Red fluorescence showed a somewhat less abrupt change at ca. 20 mol % of **2** (80 mol % of **1**). These findings suggest that the specific assemblies do not maintain their well-defined characteristics upon incorporating even a small (10-20 mol %) fraction of the other building block. (iii) In the (**1**+**3**)-system (Figure 4B), slightly different results were obtained. The fluorescence intensity measured in the Nile Red assay started to increase at lower **1**-content (60 mol % **1**) than in the (**1**+**2**)-system (80 mol% **1**). The ThT assay showed more marked differences: the fluorescent signal dropped significantly only at high **1**-content (80 mol %) in contrast to the (**1**+**2**)-system (10 mol%). We concluded that the mixed (**1**+**2**, **1**+**3**) hexamer assemblies could retain their β-sheet character even upon incorporation of large relative amounts of **1**. In contrast, the structure of the $\mathbf{1}_6$ – assemblies could not be maintained upon incorporation of the peptide building block.

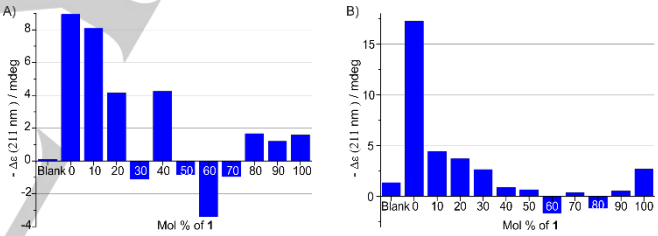

Figure 5. Ellipticity (measured at 211 nm) of DCLs containing mixed hexamers of A) **1** and **2** ([**1**]+[**2**] = 4.0 mM), B) **1** and **3** ([**1**]+[**3**] = 4.0 mM) with increasing molar percentage of **1**.

Next, we used CD spectroscopy to monitor how the supramolecular helicity of the two-component systems changes with increasing stoichiometry. Notably, $\mathbf{1}_6$ self-assembles into achiral nanostructures,[68] whereas the peptide β-sheets have a characteristic supramolecular CD signature.[60] Consequently, the measured ellipticity can be regarded as an indication of peptide-induced chiral organization in the assemblies. The CD signals characteristic of β-sheets disappeared already at 10 mol % of **1** (Figure 5, Figure S62, S63), indicating that the β-sheet fiber structure collapses even upon the incorporation of minor amounts of **1**. Notably, according to the UPLC measurements, samples prepared from 10 mol% **1** still contained significant amounts of $\mathbf{2}_6$ or $\mathbf{3}_6$ (which form chiral assemblies).[58,59] This discrepancy indicates that the pure peptide hexamers, although present in large quantities, were mainly incorporated into seemingly achiral nanostructures. Furthermore, in the (**1**+**3**)-system, the CD signal intensity started to decrease at much lower (10-20 mol %, Figure

10.1002/chem.202303837

5B) **1**-content than the ThT fluorescence intensity (80 mol %, Figure 4B), although both assays are, in priniciple, diagnostic for the same structural motif. This discrepancy can be resolved by considering that ThT might not be able to reach all β-sheet domains as these are shielded by the extensive lateral association of the (**1+3**) hexamer fibers (evident from the TEM data in Figure S59). In contrast, interaction of polarized light with the sample is less prone to yield such artifacts (i.e. CD signals reflect the global average chirality of the sample.)

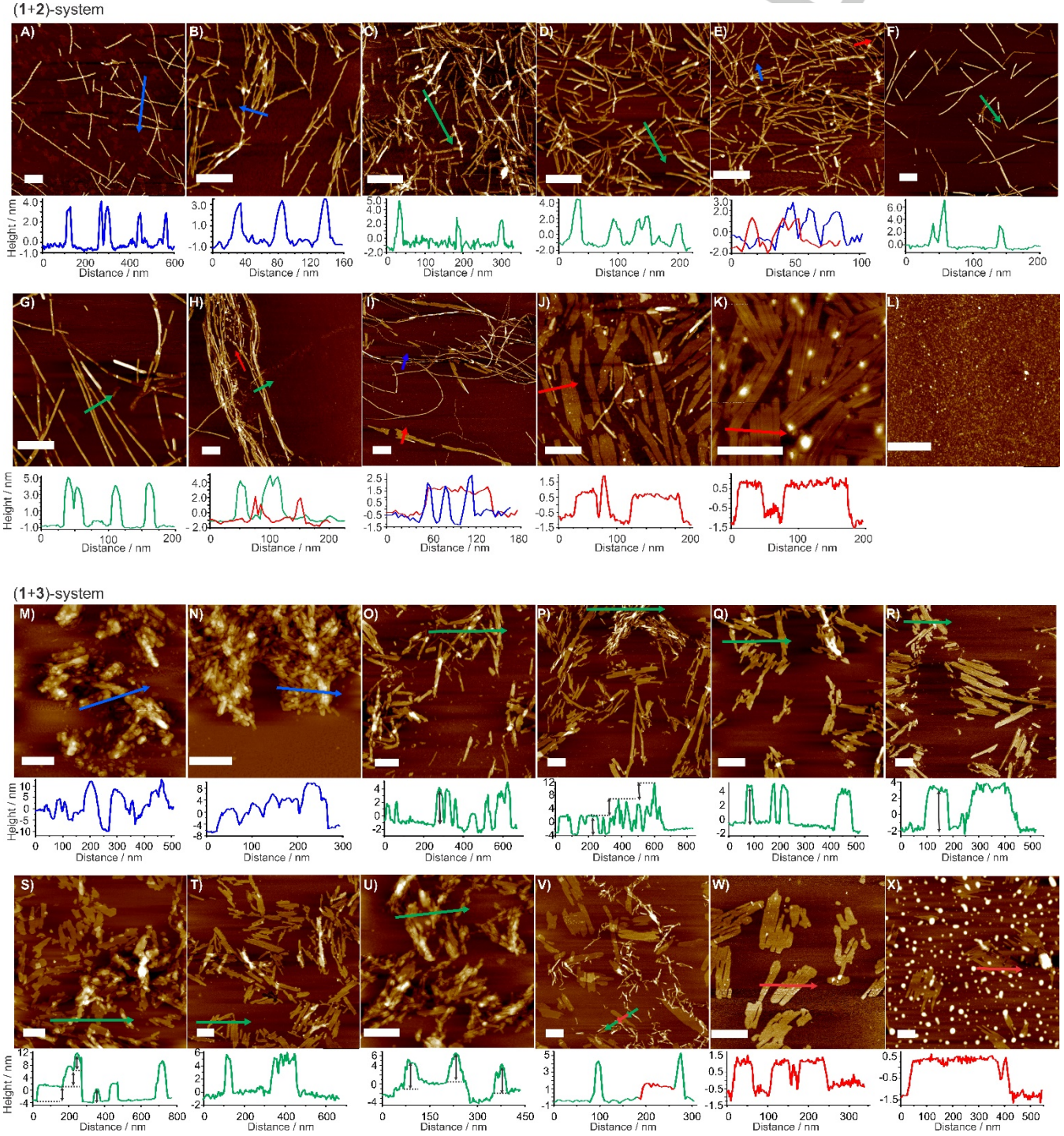

Figure 6. AFM micrographs and selected height profiles of stirred DCLs prepared from I. building blocks **1** and **2** (([**1**]+[**2**] = 4.0 mM) in aqueous borate buffer (5(mM, pH = 8.5) containing A) 0, B) 10, C) 20, D) 30, E) 40, F) 50, G) 60, H) 70, I) 80, J) 90, K) 100 mol % of building block **1** and of L) a non-stirred, oxidized DC containing 50 mol % **1**. II. building blocks **1** and **3** (([**1**]+[**3**] = 4.0 mM) in aqueous phosphate buffer (50 mM, pH = 8.5) containing M) 0, N) 5, O) 10, P) 20, Q) 30, R 40, S) 50, T) 60, U) 70, V) 80, W), 90 X) 100 mol % of building block **1**. Scale bar, 200 nm. Color code: Red: nanoribbons, Blue: chiral (helical) fibers, Green: achira fibers

10.1002/chem.202303837

Next, AFM was used in order to gain more direct insight into the changes of self-assembly modes as a function of stoichiometry (Figure 6). Previous studies showed characteristic differences between the two end points of the stoichiometric window, i.e. the pure replicators: Peptide replicators self-assemble into individual fibers (10 nm in width, 5 nm in height), which associate pairwise to give helical double fibers. [60] In contrast, **1**$_6$ self-assembles into wide nanoribbons (30-40 nm in width, 2 nm in height). [68]

Our results showed three distinct nanoscale morphologies as the relative amount of **1** is increased from 0 to 100 mol% for both systems. In case of the (**1**+**2**)-system, at very low amounts (0-10 mol%) of **1** first the expected twinned chiral fibers similar to the ones formed from **2**$_6$ were detected (Figure 6A). Next, between 20-70 mol% **1** (Figure 6C-H), the fibers displayed no apparent chirality, and their heights were more variable (2-7 nm, *vide infra*). Finally, at about 80 mol % of **1** the nanoribbons characteristic of **1**$_6$ became predominant (Figure 6I-K).

Most notably, the self-assembled structures formed from pure replicators disappear upon the incorporation of even minor amounts of the other building block. This trend corresponds to a sudden change rather than a continuous transition at the supramolecular level. In the case of **2**$_6$ (Figure 6B) this change implies the disappearance of supramolecular chirality at 10 mol% of **1** (in line with the sudden disappearance of CD signal at the same stoichiometry, see Figure 5A), although UPLC analysis indicated the presence of substantial amounts of **2**$_6$, which on its own is expected to form chiral assemblies. In other words, the morphology of the assemblies of the mixed hexamers determines the overall morphology of the sample. In the case of **1**$_6$, this rapid phase change is even more pronounced: at 80 mol% **1** (Figure 6J,V), nanoribbons are detected as objects phase-separated from the fibers (or ribbons) from mixed hexamers. Together with the fact that the fluorescence intensity in the Nile Red assay starts to increase at approximately the same stoichiometry (Figure 4A), these findings imply that most probably the detected nanoribbons are mainly composed of **1**$_6$. Thus, the **1**$_6$-nanoribbons appear to phase-separate from the assemblies of the mixed hexamers.

Furthermore, the assemblies arising from mixed (**1**+**2**)-hexamers (Figure 6C-H) show variable heights (2-7 nm) compared to those from **1**$_6$ (2 nm) or **2**$_6$ (5 nm). On the one hand, height decrease can be attributed to the incorporation of **1**-units with much shorter side chains. On the other hand, the incorporated neutral oligo(ethylene) glycol units shield the charge repulsion arising from the protonated lysine side chains of the peptide units, enabling vertical association of the fibers, which might explain the height increase compared to the pure peptide fibers. The changes in the (**1**+**3**)-system were qualitatively similar, however, with pronounced differences. Specifically, at 0-5 mol% of **1**, the supramolecular chirality of the assemblies (composed mainly of **3**$_8$ and **3**$_6$) could not be detected by AFM (Figure 6M-N), although CD spectroscopy indicated the presence of chiral, parallel β-sheets motifs (Figure 5B). This difference is most probably due to the strong vertical association of the fibers, presumably due to the higher ionic strength of the phosphate buffer used in experiments with the **1**+**3** system. Moreover, the height distribution is more irregular (between 5 and 15 nm) than for the **2**$_6$ fibers. At intermediate stoichiometries (Figure 6O-U), the irregular, vertically associated peptide fibers are replaced by more regular nanoribbons. Based on their height (5-6 nm), however, these can be clearly distinguished from the **1**$_6$-nanoribbons (height 2 nm), which appear at high (80 mol%) relative amounts of 1 (Figure 6V-X). Importantly, a quiescent sample, prepared from an equimolar amount of building blocks, was found to consist mainly of trimers and tetramers. In this sample, nanoscale assemblies were not detected by AFM (Figure 6L), suggesting that the assemblies are composed of hexamers/octamers.

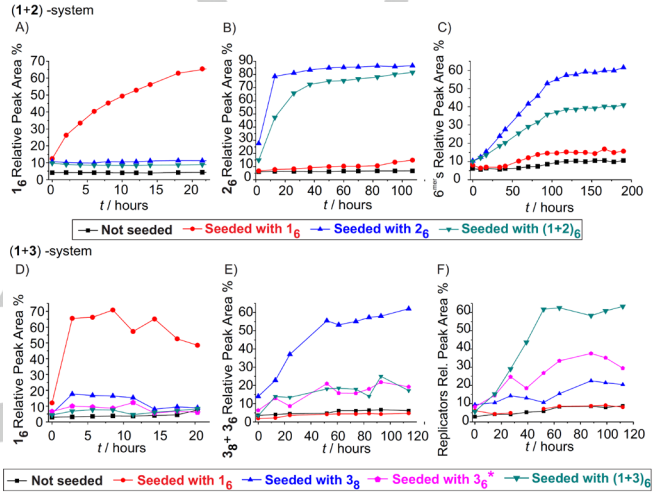

Figure 7. Comparison of self-and cross-seeding experiments, showing the time evolution of non-agitated DCLs containing A, D) **1**-food, B) **2**-food, C) (**1**+**2**)-food, E) **3**-food, F) (**1**+**3**)$_6$-food, seeded with **1**$_6$ (red circles), **2**$_6$ or **3**$_8$ (blue triangles), **3**$_6$* (purple pentagons), and (**1**+**2**)$_6$ or (**1**+**3**)$_6$ (cyan triangles) as well as a non-seeded control (black squares). Seeds denoted as **3**$_6$* are made from a 1:9 mixture of **1** and **3**.

In order to obtain precise information about the width of the assemblies, TEM measurements were carried out. Analogously to the AFM experiments, three different morphologies were observed across the stoichiometric window: strongly aggregated, 20-60 nm long and 5-15 nm wide fibers at low amounts of **1** (Figure S59A); less aggregated, 80-160 nm long and 25-50 nm wide ribbons at intermediate levels of **1** (Figure S59E-F) and several hundred (>200) nm long nanoribbons, consisting of several uniform, 6-7 nm wide stripes (Figure S59I).

These results show that the mixed systems feature three different supramolecular assembly regimes, two at the narrow extremes (5-10 and 80-100 mol% of **1**) of the stoichiometric window and one in the broad range of intermediate compositions. More importantly, the intermediate structures showed more resemblance to the peptide fibers than to the **1**$_6$ –nanoribbons.

Finally, we note that, although the bulk properties of the mixtures (fluorescence, ellipticity etc.) discussed above are somewhat variable across repeats, it is unlikely that stochasticity underlies this variability. We previously reported a two-building-block system, similar to the one described here, from which the emergence of replicators (hexamer or octamer) is stochastic, as a result of highly similar rates of nucleation of the competing replicators.[72] For the replicators studied here, nucleation rates

10.1002/chem.202303837

differ substantially: $\mathbf{1}_6$ starts to emerge in 8-9 hours,[68] whereas $\mathbf{2}_6$ and $\mathbf{3}_8$ only emerge after several days.[58]

Cross-catalytic relations reveal two generalist and one specialist replicator set. The spectroscopy and microscopy experiments described in the previous sections allowed us to distinguish three sets of replicators according to their supramolecular organizations: peptide ($\mathbf{2}_6$ or $\mathbf{3}_8$) fibers, mixed fibers lacking apparent chiral organization and $\mathbf{1}_6$ –nanoribbons. The above results suggest that, due to the similarity in geometry, peptide fibers and apparently achiral fibers might be able to grow in the same, peptide-rich food niches, whereas $\mathbf{1}_6$ does not. In other words, the two former ones are expected to be generalist replicators, whereas the latter one is expected to be a specialist.

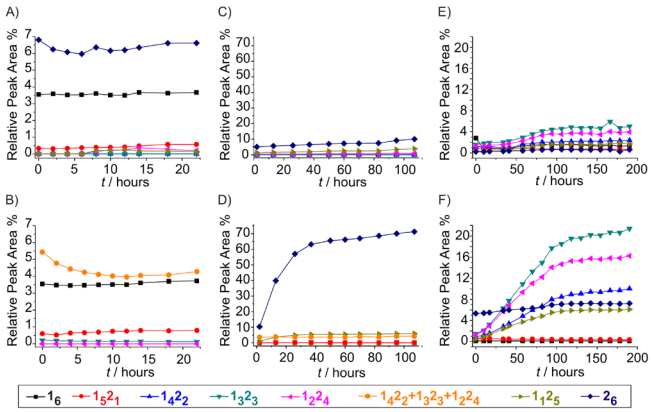

Figure 8. Time evolution of cross-seeded DCLs, showing the relative change in the concentrations of the individual replicators: A) **1**-food and $\mathbf{2}_6$-seed, B) **1**-food and $(\mathbf{1+2})_6$-seed, C) **2**-food and $\mathbf{1}_6$-seed D) **2**-food and $(\mathbf{1+2})_6$-seed, E) $(\mathbf{1+2})$-food and $\mathbf{1}_6$-seed, F) $(\mathbf{1+2})$-food and $\mathbf{2}_6$-seed.

In order to test this hypothesis, self- and cross-seeding experiments were carried out. In these experiments, partially oxidized samples containing mainly trimers and tetramers (food) were mixed with 10 mol% of replicator (seed). The amount of replicators formed via the seed-catalyzed pathway was measured by UPLC and was taken as a direct measure of auto- or cross-catalytic efficiency of a given replicator in a certain food niche. As spontaneous replicator emergence is mechanosensitive, the samples were not agitated in order to ensure that hexamer formation solely results from the catalytic effect of the added seed. Three different food samples were used in each system: **1**-food, **2**-food and (**1**+**2**)-food (prepared by oxidation of **1**, **2** and an equimolar mixture of the two building blocks) in the (**1**+**2**)-system, as well as **1**-food, **3**-food and (**1**+**3**)-food in the (**1**+**3**)-system (prepared in an analogous manner). In the case of the (**1**+**2**)-system, three corresponding seeds were used: $\mathbf{1}_6$, $\mathbf{2}_6$ and $(\mathbf{1+2})_6$ (the latter was composed of hexamers prepared from an equimolar mixture of **1** and **2**). In the (**1**+**3**)-system, besides the analogous $\mathbf{1}_6$, $\mathbf{3}_8$ and $(\mathbf{1+3})_6$ seeds, an additional seed prepared from a 1:9 mixture of **1** and **3** was used (denoted $\mathbf{3}_6$*). The latter seed, containing mainly $\mathbf{3}_6$ as replicating species, was designed in order to distinguish between macrocycle size and replicator identity as decisive factors in cross-catalytic efficiency. Details on the seeding experiments can be found in Section 3 of the Supporting Information.

The results show that the hexamer peptide replicators and the mixed replicators were mutually cross-catalytic, but they did not cross-catalyze the formation of $\mathbf{1}_6$ (Figure 7B-C, E-F). Correspondingly, $\mathbf{1}_6$ is not cross-catalytic toward either the peptide or the mixed replicators (Figure 7A, D). Finally, as expected, all seeds catalyzed their own formation from their corresponding food niches.

The mutual cross-seeding abilities of $\mathbf{2}_6$ and $(\mathbf{1+2})_6$ can be rationalized by their closely related morphologies (similar fiber width) and the similar intermolecular binding motif (oriented peptide-peptide interactions). By the same logic, the ineffective cross-seeding between $\mathbf{1}_6$ and the other two replicators can be attributed to a mismatch in packing mode and/or in the strength of secondary interactions holding together the assemblies. Interestingly, $\mathbf{2}_6$ outperforms $(\mathbf{1+2})_6$ both as an auto – and as a cross-catalyst, (Figure 7B-C), probably because the interaction strength between catalytic fiber ends and incoming food molecules is higher for $\mathbf{2}_6$ than for $(\mathbf{1+2})_6$ due to the higher number and directionality of binding sites in the former.

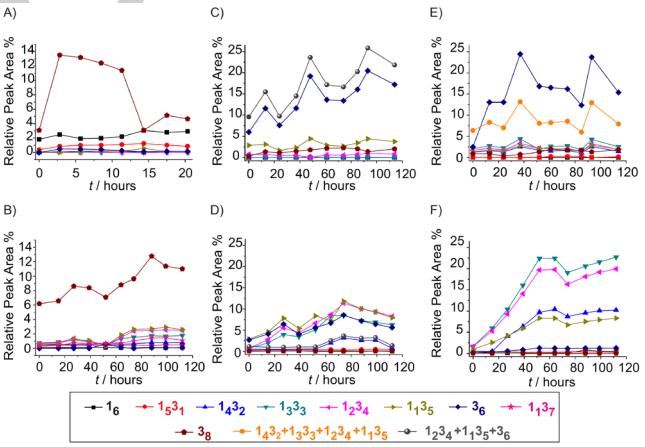

Figure 9. Time evolution of cross-seeded DCLs, showing the relative change in the concentrations of the individual replicators: A) **1**-food and $\mathbf{3}_8$-seed, B) $(\mathbf{1+3})$-food and $\mathbf{3}_8$-seed, C) **3**-food and $\mathbf{3}_6$*-seed D) $(\mathbf{1+3})$-food and $\mathbf{3}_6$*-seed, E) **3**-food and $(\mathbf{1+3})_6$-seed, F) $(\mathbf{1+3})$-food and $(\mathbf{1+3})_6$-seed. Seeds denoted as $\mathbf{3}_6$* are made from a 1:9 mixture of **1** and **3**.

Detailed examination of the time evolution of the individual hexamer macrocycles during cross-seeding experiments revealed analogous trends (Figure 8 and Figure 9). In the (**1**+**2**)-system, $\mathbf{1}_6$-seed rapidly disintegrated in the presence of **2**- and (**1**+**2**)-food (Figure 8C,E, Figure S66C,D black squares), re-equilibrating to trimers and tetramers. In contrast, $\mathbf{2}_6$- (Figure 8A, F, blue diamonds) and $(\mathbf{1+2})_6$-seed (Figure 8B, D, orange circles, amount calculated from the total concentration of its main components, i.e. $[\mathbf{1}_3\mathbf{2}_3] + [\mathbf{1}_4\mathbf{2}_2] + [\mathbf{1}_2\mathbf{2}_4]$) persisted in the presence of non-self food. It should be noted that generally, the formation of a large number of smaller macrocycles (i.e. formation of trimers and tetramers) is entropically preferred to that of a smaller number of bigger macrocycles, [73,74] as shown for the $\mathbf{1}_6$ -seed. However,

10.1002/chem.202303837

if the overall interaction strength between the macrocycles of the seed assemblies is sufficiently large, it may counterbalance the entropy-driven process, as shown for the **2**$_6$- and (**1**+**2**)$_6$-seeds.

In the (**1**+**3**)-system, peptide-containing hexamer replicators were able to grow in peptide-containing food niches with different compositions, although to a lesser extent (Figure 9C-E). In contrast, octamer replicator **3**$_8$ could only replicate in its own food niche (Figure 7E), and although it persisted (but barely replicated) in the presence of (**1**+**3**)-food (Figure 9B), it disintegrated in the presence of **1**-food, without giving rise to mixed octamers (Figure 9A). In other words, no significant cross-catalysis took place between replicators of different ring sizes.

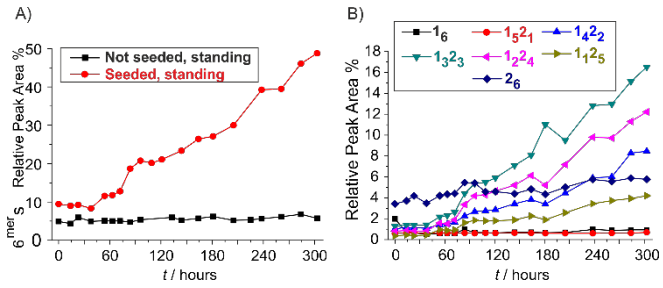

Figure 10. Time evolution of DCLs prepared from (**1**+**2**)-food ([**1**] = [**2**] = 2.0 mM) and seeded with equimolar amounts of **1**$_6$ and **2**$_6$ (10 mol% each) in the absence of stirring. Time evolution of the A) total mol% of hexamers (compared to a non-seeded control); B) mol% of each hexamer in the seeded sample.

Taken together, these results (Table 1) indicate that **1**$_6$ (and **3**$_8$) are specialist replicators as they can grow only in food niches that corresponds to their exact composition. In contrast, peptide-containing hexamer replicators are generalists as they are able to grow in food niches whose composition are markedly different from their own (but contain sufficient food for their growth). We thus designed a scenario where a specialist and a generalist replicator compete with each other for nutrients in the presence of a food which contains building blocks for both replicators. To this end, we prepared (**1**+**2**)-food ([**1**]=[**2**]=2.0 mM) and seeded it simultaneously with **1**$_6$- and **2**$_6$-seed (10 mol% each) in the absence of stirring. Hexamer growth was observed, as compared to the non-seeded control (Figure 10A). The kinetic profile was similar to the case when only **2**$_6$-seed was used. Most notably, **1**$_6$ again disintegrated rapidly, showing that for this particular system, specialist and generalist species do not modulate the behavior of each other when both are present in the same sample (Figure 10B).

Table 1. Auto- and cross-catalytic relationships between replicators A) **1**$_6$, **2**$_6$ and **(1+2)**$_6$; **B) 1**$_6$, **3**$_8$, **3**$_6$* and **(1+3)**$_6$. Empty = no catalytic relationship; blue = positive catalytic relationship, preservation of food and seed stoichiometry; red = positive catalytic relationship, loss of either food or seed stoichiometry

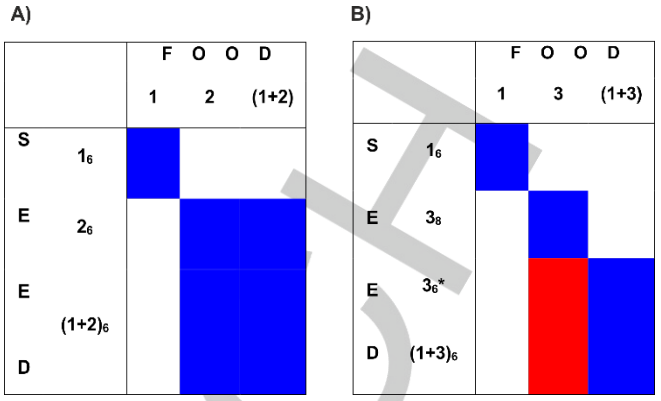

We observed that information at the molecular level cannot be transferred in seeding experiments, i.e. in cross-seeding experiments using (**1**+**2**)-food, the final hexamer distribution was similar regardless of the seed used (Figure S64). We were interested whether the same trend holds at the supramolecular level. We used fiber chirality as an indicator of supramolecular organization and investigated whether chirality can be transferred from chiral seeds to food molecules that otherwise would give rise to replicator assemblies with no apparent supramolecular chirality. In the sample prepared by cross-seeding (**1**+**2**)-food with **2**$_6$-seed (Figure 8F) mainly chiral fibers were observed (Figure S65C), although the (**1**+**2**)$_6$-replicators were shown to assemble into apparently achiral fibers (Figure 6C-H), in the absence of seed. In contrast, seeding **2**-food with (**1**+**2**)$_6$-seed, only achiral fibers were detected (Figure S65B). These results show that the information at the supramolecular level can be transferred during seeding experiments. Note that we previously reported that molecular-level chirality was not transferred during replication of **2**$_6$, while it was heritable for replicator **2**$_5$ which has a somewhat smaller ring size, but also a different mode of assembly.[75] These observations provide further support for the notion that the mode of supramolecular organization strongly influences the extent of chiral information transfer. Work is currently ongoing on further exploring emergence and transfer of chiral information in self-replicating systems.

Conclusions

In summary, we investigated what determines whether self-replicators are specialists or generalists in a simple system of replicators based on oligo(ethylene glycol)-conjugated building block **1** and peptide building blocks **2** or **3**. Equimolar mixtures of **1** and either **2** or **3** gave rise to mixed hexamer replicators. Based on their supramolecular morphology, the assemblies of mixed replicators are different from those composed of pure replicators, therefore can be regarded as a distinct set of species. Most importantly, auto- and cross-seeding experiments showed that the peptide-containing hexamer replicators (both pure and mixed) are generalists, i.e. they are able to replicate in at least two very different food niches, whereas non-peptide hexamer **1**$_6$ and peptide octamer **3**$_8$ are specialists, i.e. they replicate only in a very specific food niche which is based solely on their constituent

building blocks (Table 1). Whether replicators are generalists or specialists depends strongly on the supramolecular organization of the replicators, which, in turn, is likely related to the interaction strength between the building blocks from which they are composed: assemblies from strongly interacting building blocks appear more forgiving towards the incorporation of other building blocks, leading to generalist replicators, while more weakly interacting building blocks yield replicators that are less resilient to incorporation of structurally different building blocks, yielding specialist replicators.

Synthetic replicators that can demonstrate Darwinian evolution based on generalist/specialist behavior are still several steps away. Although we recently demonstrated out-of-equilibrium complexification of synthetic replicators,[76] the system described there was based on only one building block. Generalist replicators, on the other hand, by definition, incorporate multiple building blocks. This, in turn, would render heredity of information (building block sequence) difficult, due to the high number of possible macrocycle compositions in the case of even a low number of building blocks. Sequence specificity, i.e. the preferred formation of a macrocycle with a given sequence (or even stoichiometry) of building blocks is needed to overcome this obstacle. Sequence specificity in disulfide macrocycles has recently been demonstrated but either the sequence-specifically formed macrocycles were not self-replicators[77] or their molecular complexity was relatively low.[78] Sequence-specific replicator formation (via supramolecular interactions pre-programmed in the structure of the building blocks), together with large differences in the kinetics (length of lag phase) and/or thermodynamics (strength of secondary interactions holding together the assemblies) of self-replication would pave the way towards generalist replicators with reliable heredity of sequence information, and toward their Darwinian evolution.

Experimental Section

The syntheses of building blocks **1**,[68] **2** and **3**[53,58] were reported previously. Experimental details on the preparation (including seeding experiments) and analysis (UPLC, LC-MS, fluorescence spectroscopy, CD spectroscopy, AFM, TEM) of the libraries is described in the Supporting Information.

Acknowledgements

We are grateful for ERC (Advanced Grant Nr 741774), the NWO and COST action CM-1304 for financial support. D. K. thanks György Barabás (Univeristy of Linköping, Sweden) for fruitful discussions.

Keywords: self-replication • systems chemistry • dynamic combinatorial chemistry • generalist species • specialist species

[1] J.-M. Lehn, *Supramolecular Chemistry*, Wiley, **1995**.

[2] C. R. Bertozzi, *ACS Cent. Sci.* **2015**, *1*, 1–2.

[3] J.-M. Lehn, *Angew. Chem. Int. Ed.* **2015**, *54*, 3276–3289.

[4] R. F. Ludlow, S. Otto, *Chem. Soc. Rev.* **2008**, *37*, 101–108.

[5] K. Ruiz-Mirazo, C. Briones, A. de la Escosura, *Chem. Rev.* **2014**, *114*, 285–366.

[6] M. Kreysing, L. Keil, S. Lanzmich, D. Braun, *Nat. Chem.* **2015**, *7*, 203–208.

[7] T. P. Kee, P.-A. Monnard, *Beilstein J. Org. Chem* **2017**, *13*, 1551–1563.

[8] L. M. Barge, *Nat. Commun.* **2018**, *9*, 5170.

[9] S. Asche, G. J. T. Cooper, G. Keenan, C. Mathis, L. Cronin, *Nat. Commun.* **2021**, *12*, 3547

[10] C. E. Cleland, C. F. Chyba, *Orig. Life Evol. Biosph.* **2002**, *32*, 387–393.

[11] P. L. Luisi, F. Ferri, P. Stano, *Naturwissenschaften* **2006**, *93*, 1–13.

[12] T. Gánti, *The Principles of Life*, Oxford University Press, **2003**.

[13] S. Otto, *Acc. Chem. Res.* **2022**, *55*, 145–155.

[14] G. von Kiedrowski, *Angew. Chem. Int. Ed.* **1986**, *25*, 932–935.

[15] T. Tjivikua, P. Ballester, J. Rebek, *J. Am. Chem. Soc.* **1990**, *112*, 1249–1250.

[16] D. H. Lee, J. R. Granja, J. A. Martinez, K. Severin, M. R. Ghadiri, *Nature* **1996**, *382*, 525–528.

[17] E. Kassianidis, D. Philp, *Angew. Chem. Int. Ed.* **2006**, *45*, 6344–6348.

[18] T. Kosikova, N. I. Hassan, D. B. Cordes, A. M. Z. Slawin, D. Philp, *J. Am. Chem. Soc.* **2015**, *137*, 16074–16083.

[19] J. W. Sadownik, D. Philp, E. A. Wood, D. Philp, J. J.-P. Peyralans, S. Otto, R. M. Kellogg, B. Kaptein, E. Vlieg, D. G. Blackmond, *Org. Biomol. Chem.* **2015**, *13*, 10392–10401.

[20] G. Clixby, L. Twyman, *Org. Biomol. Chem.* **2016**, *14*, 4170–4184.

[21] T. Kosikova, D. Philp, *Chem. Soc. Rev.* **2017**, *46*, 7274–7305.

[22] J. W. Sadownik, T. Kosikova, D. Philp, *J. Am. Chem. Soc.* **2017**, *139*, 17565–17573.

[23] P. Stano, P. L. Luisi, *Chem. Commun.* **2010**, *46*, 3639–3653.

[24] C. B. Minkenberg, F. Li, P. van Rijn, L. Florusse, J. Boekhoven, M. C. A. Stuart, G. J. M. Koper, R. Eelkema, J. H. van Esch, *Angew. Chem. Int. Ed.* **2011**, *50*, 3421–3424.

[25] K. Kurihara, M. Tamura, K. Shohda, T. Toyota, K. Suzuki, T. Sugawara, *Nat. Chem.* **2011**, *3*, 775–781.

[26] P. Stano, P. L. Luisi, *Curr. Opin. Biotechnol.* **2013**, *24*, 633–638.

[27] K. Kurihara, Y. Okura, M. Matsuo, T. Toyota, K. Suzuki, T. Sugawara, *Nat. Commun.* **2015**, *6*, 8352.

[28] L. J. Points, J. W. Taylor, J. Grizou, K. Donkers, L. Cronin, *Proc. Natl. Acad. Sci. U. S. A.* **2018**, *115*, 885–890.

[29] M. Abbas, W. P. Lipiński, J. Wang, E. Spruijt, *Chem. Soc. Rev.* **2021**, *50*, 3690–3705.

[30] J. A. Vance, N. K. Devaraj, *J. Am. Chem. Soc.* **2021**, *143*, 8223–8231.

[31] R. Mizuuchi, N. Ichihashi, *Life* **2021**, *11*, 191.

[32] J. Ottelé, A. S. Hussain, C. Mayer, S. Otto, *Nat. Catal.* **2020**, *3*, 547–553.

[33] G. Monreal Santiago, K. Liu, W. R. Browne, S. Otto, *Nat. Chem.* **2020**, *12*, 603–607.

[34] E. Mattia, S. Otto, *Nat. Nanotechnol.* **2015**, *10*, 111–119.

[35] B. A. Grzybowski, K. Fitzner, J. Paczesny, S. Granick, *Chem. Soc.*

Rev. **2017**, *46*, 5647–5678.

[36] H. Hess, J. L. Ross, *Chem. Soc. Rev.* **2017**, *46*, 5570–5587.

[37] M. Tena-Solsona, C. Wanzke, B. Riess, A. R. Bausch, J. Boekhoven, *Nat. Commun.* **2018**, *9*, 2044.

[38] J. Leira-Iglesias, A. Tassoni, T. Adachi, M. Stich, T. M. Hermans, *Nat. Nanotechnol.* **2018**, *13*, 1021–1027.

[39] I. Maity, N. Wagner, R. Mukherjee, D. Dev, E. Peacock-Lopez, R. Cohen-Luria, G. Ashkenasy, *Nat. Commun.* **2019**, *10*, 4636.

[40] M. Weißenfels, J. Gemen, R. Klajn, *Chem* **2021**, *7*, 23–37.

[41] C. Donau, F. Späth, M. Sosson, B. A. K. Kriebisch, F. Schnitter, M. Tena-Solsona, H. S. Kang, E. Salibi, M. Sattler, H. Mutschler, J. Boekhoven, *Nat. Commun.* **2020**, *11*, 5167.

[42] B. Rieß, R. K. Grötsch, J. Boekhoven, *Chem* **2020**, *6*, 552–578.

[43] K. Ruiz-Mirazo, J. Umerez, A. Moreno, *Biol. Philos.* **2007**, *23*, 67–85.

[44] J. M. P. Gutierrez, T. Hinkley, J. W. Taylor, K. Yanev, L. Cronin, *Nat. Commun.* **2014**, *5*, 5571.

[45] H. Duim, S. Otto, *Beilstein J. Org. Chem.* **2017**, *13*, 1189–1203.

[46] K. Liu, A. Blokhuis, C. van Ewijk, A. Kiani, J. Wu, W. H. Roos, S. Otto, *Nat. Chem.* **2024**, *16*, 79–88,

[47] P. Nghe, W. Hordijk, S. A. Kauffman, S. I. Walker, F. J. Schmidt, H. Kemble, J. A. M. Yeates, N. Lehman, *Mol. Biosyst.* **2015**, *11*, 3206–3217.

[48] J. A. M. Yeates, C. Hilbe, M. Zwick, M. A. Nowak, N. Lehman, *Proc. Natl. Acad. Sci. U. S. A.* **2016**, *113*, 5030–5035.

[49] D. H. Lee, K. Severin, Y. Yokobayashi, M. R. Ghadiri, *Nature* **1997**, *390*, 591–594.

[50] N. Vaidya, M. L. Manapat, I. A. Chen, R. Xulvi-Brunet, E. J. Hayden, N. Lehman, *Nature* **2012**, *491*, 72–77.

[51] C. R. Townsend, M. Begon, J. L. Harper, *Essentials of Ecology*, Blackwell Publishing, Oxford, **2008**.

[52] P. Adamski, M. Eleveld, A. Sood, Á. Kun, A. Szilágyi, T. Czárán, E. Szathmáry, S. Otto, *Nat. Rev. Chem. 2020 48* **2020**, *4*, 386–403.

[53] J. M. A. Carnall, C. A. Waudby, A. M. Belenguer, M. C. A. Stuart, J. J.-P. Peyralans, S. Otto, *Science* **2010**, *327*, 1502–1506.

[54] J. Li, P. Nowak, S. Otto, *J. Am. Chem. Soc.* **2013**, *135*, 9222–9239.

[55] Y. Jin, C. Yu, R. J. Denman, W. Zhang, *Chem. Soc. Rev.* **2013**, *42*, 6634–6654.

[56] W. Zhang, Y. Jin, *Dynamic Covalent Chemistry : Principles, Reactions, and Applications*, Wiley, **2018**.

[57] S. P. Black, J. K. M. Sanders, A. R. Stefankiewicz, *Chem. Soc. Rev.* **2014**, *43*, 1861–1872.

[58] M. Malakoutikhah, J. J.-P. Peyralans, M. Colomb-Delsuc, H. Fanlo-Virgós, M. C. A. Stuart, S. Otto, *J. Am. Chem. Soc.* **2013**, *135*, 18406–18417.

[59] G. Leonetti, S. Otto, *J. Am. Chem. Soc.* **2015**, *137*, 2067–2072.

[60] P. W. J. M. Frederix, J. Idé, Y. Altay, G. Schaeffer, M. Surin, D. Beljonne, A. S. Bondarenko, T. L. C. Jansen, S. Otto, S. J. Marrink, *ACS Nano* **2017**, *11*, 7858–7868.

[61] M. Colomb-Delsuc, E. Mattia, J. W. Sadownik, S. Otto, *Nat. Commun.* **2015**, *6*, 7427.

[62] P. Nowak, M. Colomb-Delsuc, S. Otto, J. Li, *J. Am. Chem. Soc.* **2015**, *137*, 10965–10969.

[63] D. Komáromy, M. Tezcan, G. Schaeffer, I. Marić, S. Otto, *Angew. Chem. Int. Ed.* **2017**, *56*, 14658–14662.

[64] B. Bartolec, M. Altay, S. Otto, *Chem. Commun.* **2018**, *54*, 13096–13098.

[65] J. W. Sadownik, E. Mattia, P. Nowak, S. Otto, *Nat. Chem.* **2016**, *8*, 264–269.

[66] Y. Altay, M. Tezcan, S. Otto, *J. Am. Chem. Soc.* **2017**, *139*, 13612–13615.

[67] M. Altay, Y. Altay, S. Otto, *Angew. Chem. Int. Ed.* **2018**, *57*, 10564–10568.

[68] D. Komáromy, M. C. A. Stuart, G. Monreal Santiago, M. Tezcan, V. V. Krasnikov, S. Otto, *J. Am. Chem. Soc.* **2017**, *139*, 6234–6241.

[69] B. Rubinov, N. Wagner, M. Matmor, O. Regev, N. Ashkenasy, G. Ashkenasy, *ACS Nano* **2012**, *6*, 7893–7901.

[70] A. Pal, M. Malakoutikhah, G. Leonetti, M. Tezcan, M. Colomb-Delsuc, V. D. Nguyen, J. van der Gucht, S. Otto, *Angew. Chem. Int. Ed.* **2015**, *54*, 7852–7856.

[71] P. Greenspan, *J. Cell Biol.* **1985**, *100*, 965–973.

[72] G. Schaeffer, M. J. Eleveld, J. Ottele, P. C. Kroon, P. W. J. M. Frederix, S. Yang, S. Otto, *J. Am. Chem. Soc.* **2022**, *144*, 6291–6297.

[73] K. Severin, *Chem. Eur. J.* **2004**, *10*, 2565–2580.

[74] P. T. Corbett, J. K. M. Sanders, S. Otto, *J. Am. Chem. Soc.* **2005**, *127*, 9390–9392.

[75] S. Yang, Y. Geiger, M. Geerts, M. J. Eleveld, A. Kiani, S. Otto, *J. Am. Chem. Soc.* **2023**, *145*, 16889–16898.

[76] S. Yang, G. Schaeffer, E. Mattia, O. Markovitch, K. Liu, A. S. Hussain, J. Ottelé, A. Sood, S. Otto, *Angew. Chem. Int. Ed.* **2021**, *60*, 11344–11349.

[77] D. Komáromy, T. Tiemersma-Wegman, J. Kemmink, G. Portale, P. R. Adamski, A. Blokhuis, F. S. Aalbers, I. Marić, G. M. Santiago, J. Ottelé, A. Sood, V. Saggiomo, B. Liu, P. van der Meulen, S. Otto, *Chem* **2021**, *7*, 1933–1951.

[78] B. Liu, C. G. Pappas, J. Ottelé, G. Schaeffer, C. Jurissek, P. F. Pieters, M. Altay, I. Marić, M. C. A. Stuart, S. Otto, *J. Am. Chem. Soc.* **2020**, *142*, 4184–4192.

10.1002/chem.202303837

WILEY-VCH

FULL PAPER

Entry for the Table of Contents

FULL PAPER

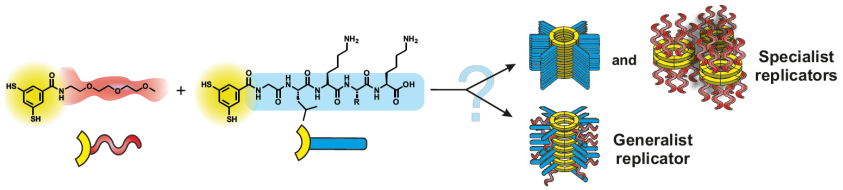

Dávid Komáromy, Diego M. Monzón, Ivana Marić, Guillermo Monreal Santiago, Jim Ottelé, Meniz Altay, Gaël Schaeffer, and Sijbren Otto*

Page No. – Page No.

Generalist versus Specialist Self-Replicators

Whether assembly-driven self-replicators that emerge from a mixture of two building blocks specialize on one resource or are generalists was found to depend on their supramolecular organization.

Institute and researcher Twitter usernames:
David Komaromy: @seilenfranzli
Ivana Marić @Nitrogeno_N
Guillermo Monreal Santiago: @GuilleMonrealS
Sijbren Otto: @OttoLab
Stratingh Institute for Chemistry: @StratinghInst

[a] D. Komáromy, I. Marić, G. Monréal Santiago, J. Ottelé, M. G. Schaeffer and Prof. Dr. S. Otto
University of Groningen, Centre for Systems Chemistry, S